Supporting Information

Solid-phase synthesis and evaluation of tumour-targeting phenylboronate-based MRI contrast agents

Jonathan Martinelli,[a,b] Rogelio Jiménez-Juárez,[a,c] Diego Alberti,[d] Simonetta Geninatti Crich,[d] and Kristina Djanashvili*[,a]

[a] Department of Biotechnology, Delft University of Technology, Van der Maasweg 9, 262 HZ Delft, The Netherlands

[b] Department of Science and Technological Innovation, Università del Piemonte Orientale, Viale Michel 11, 15121 Alessandria, Italy

[c] Department of Organic Chemistry, National School of Biological Sciences, National Polytechnical Institute, Prolongación de Carpio y Plan de Ayala S/N, 11340, Mexico D.F., Mexico

[d] Department of Molecular Biotechnology and Health Sciences, University of Torino, via Nizza 52, Torino, Italy

Table of contents

1. pKa's Determination

^{11}B NMR-titration measurements were performed on Varian INOVA-300 spectrometers at 96.3 MHz and 25 °C using 5 mm NMR sample tubes. A 0.1 M solution of H_3BO_3 in D_2O (δ = 0.00 ppm) was used as external reference. The conversion to the $BF_3{\cdot}Et_2O$ scale by -18.7 ppm was applied. About 240 scans were collected using a delay and an acquisition time of 1 s. Boron-containing compounds were dissolved in a water (10% D_2O) / methanol (2:1 v/v) mixture. The pH values of the samples were measured at 25 °C with a Corning 125 pH-meter using a calibrated micro-combination probe purchased from Sigma Aldrich. The pH values were adjusted with 1 M solutions of NaOH and HCl.

The resonance of ^{11}B within the entire range of pH studied showed transition of B-atom from its planar B^0 (sp^2-hybridized) configuration at lower pH to the tetragonal B^- (sp^3-hybridized) configuration upon increase of the pH. With the exchange between B^0 and B^- being rapid on the ^{11}B NMR time-scale, the average chemical shift and the ionization constant of boron can be defined by the eqs. (1) and (2), where χ_i is the molar fraction of B^0 and B^- and δ is the corresponding chemical shift. Fitting the experimental data to eqs (1) and (2) allowed for calculation of the pKa values of the corresponding compounds.

$$\delta = \sum_i \chi_i \delta_i \qquad (1)$$

$$K_a = \frac{[B^-][H^+]}{[B^0]} \qquad (2)$$

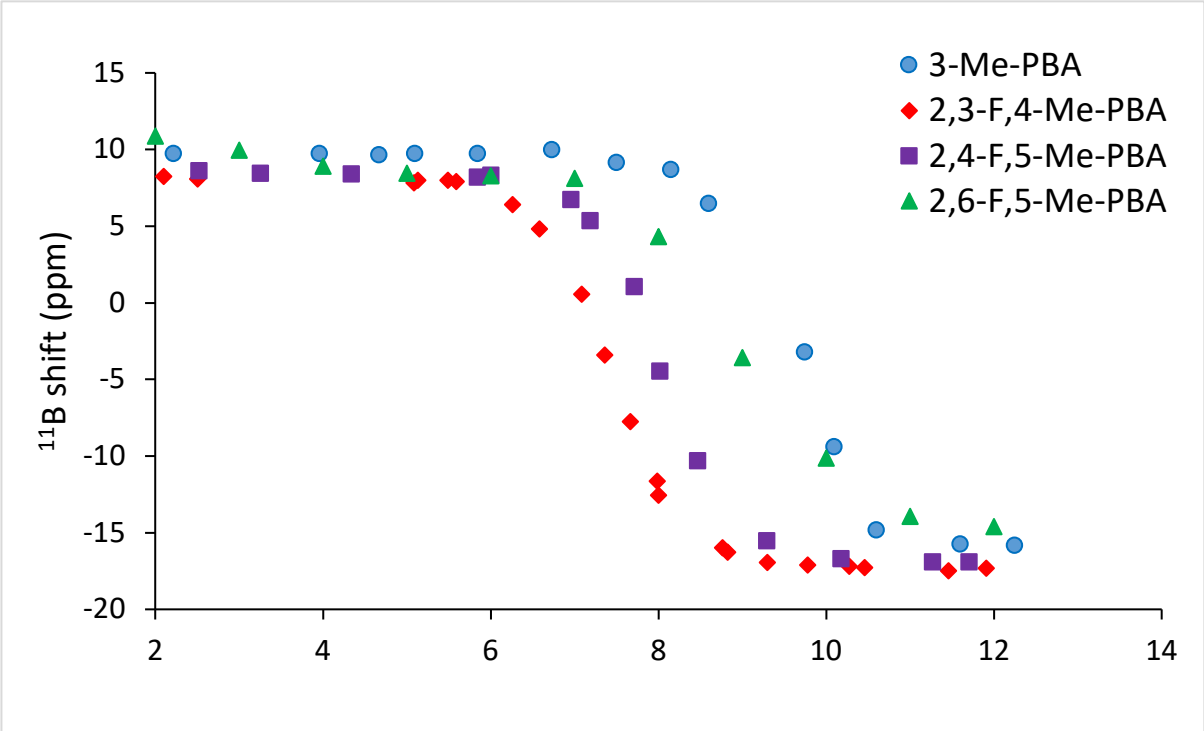

Figure S1. pH profiles of the ^{11}B chemical shift of a solution of PBA-containing model compounds.

pKa (3-Me-PBA) = 8.8

pKa (2,3-F-4-Me-PBA) = 7.2

pKa (2,4-F-5-Me-PBA) = 8.0

pKa (2,6-f-5-Me-PBA) = 8.6

2. HPLC- and ESI-MS

Analytical HPLC gradient conditions for DOTA-EN-F2PBA:

Solvent A: H_2O TFA 0.1%; Solvent B: ACN TFA 0.1%; Flow: 1 ml/min; t_R = 11.7 min

Time (min)	Solvent A (%)	Solvent B (%)
0	90	10
2,00	90	10
16,00	0	100
19,00	0	100

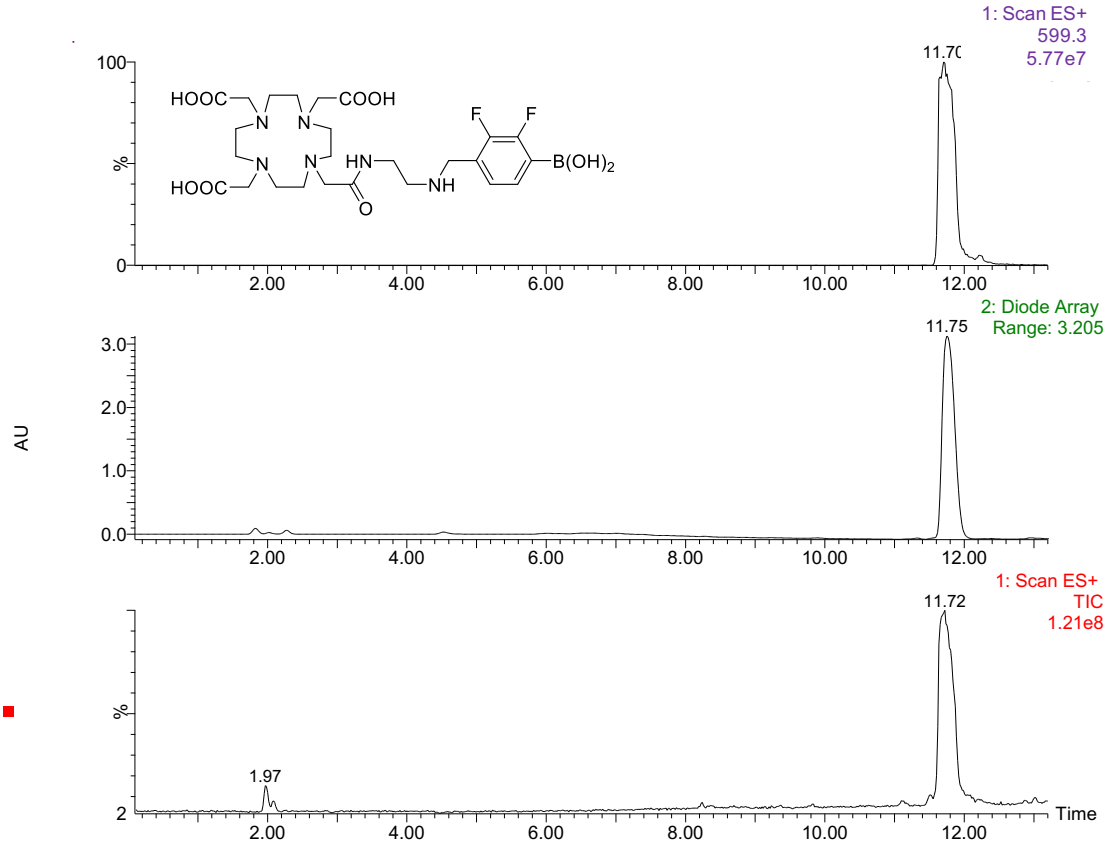

Figure S2. ESI^+ MS (*bottom*), UV (254 nm, *middle*) and specific ion ($M\text{-}H_2O+H^+$, *top*) HPLC chromatograms of DOTA-EN-F2PBA from solid-phase synthesis (the peak at 2.0 min is due to the solvent front).

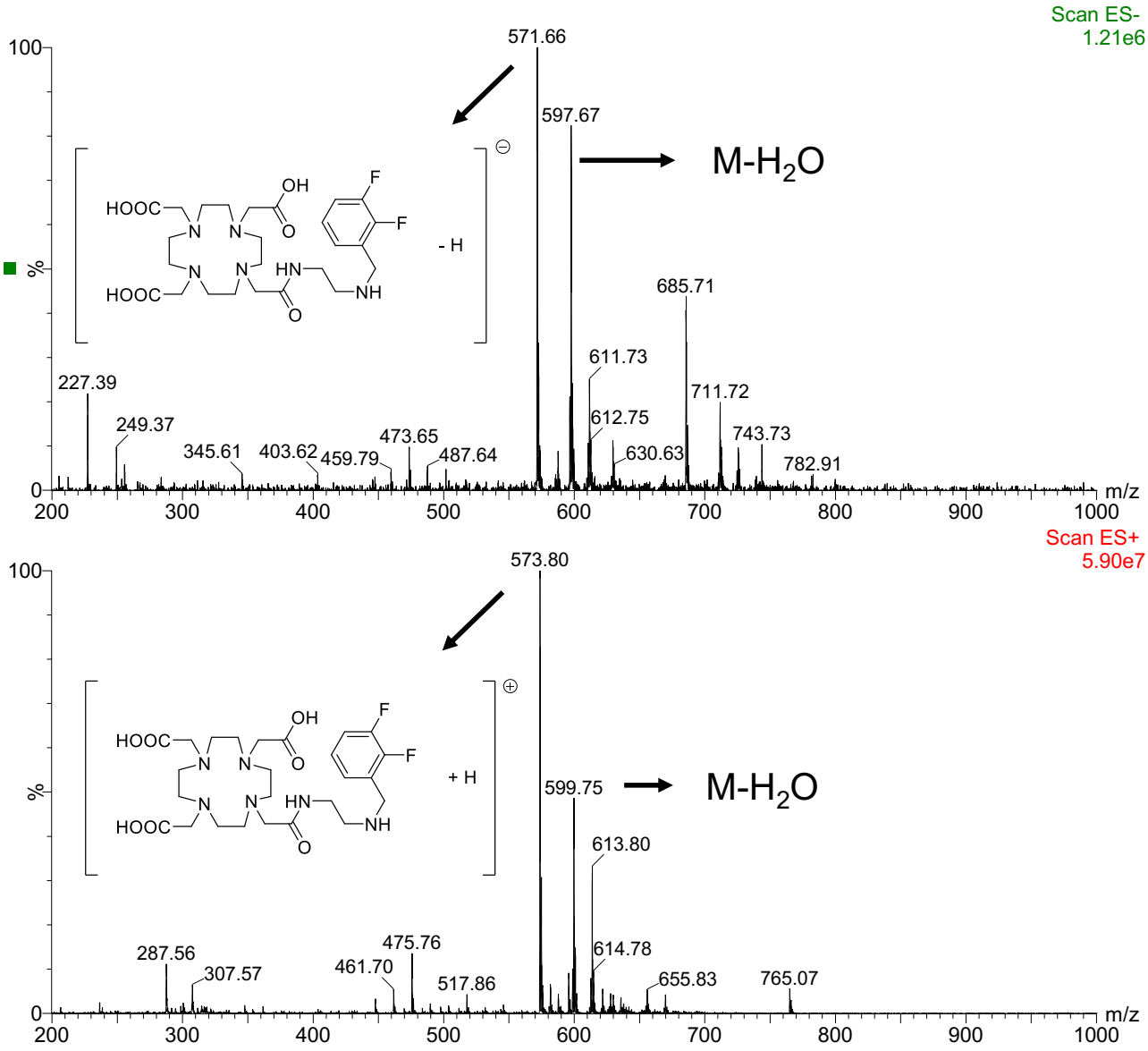

Figure S3. ESI$^-$ (*top*) and ESI$^+$ (*bottom*) mass spectra of DOTA-EN-F2PBA ligand prepared in solution. The peaks at 571.7 (negative mode) and 573.8 (positive mode) m/z correspond to the deboronated by-product. M^+ = 616.3 m/z; M-H_2O+H^+ = 599.3 m/z; M-$B(OH)_2$+H^+ = 573.3 m/z.

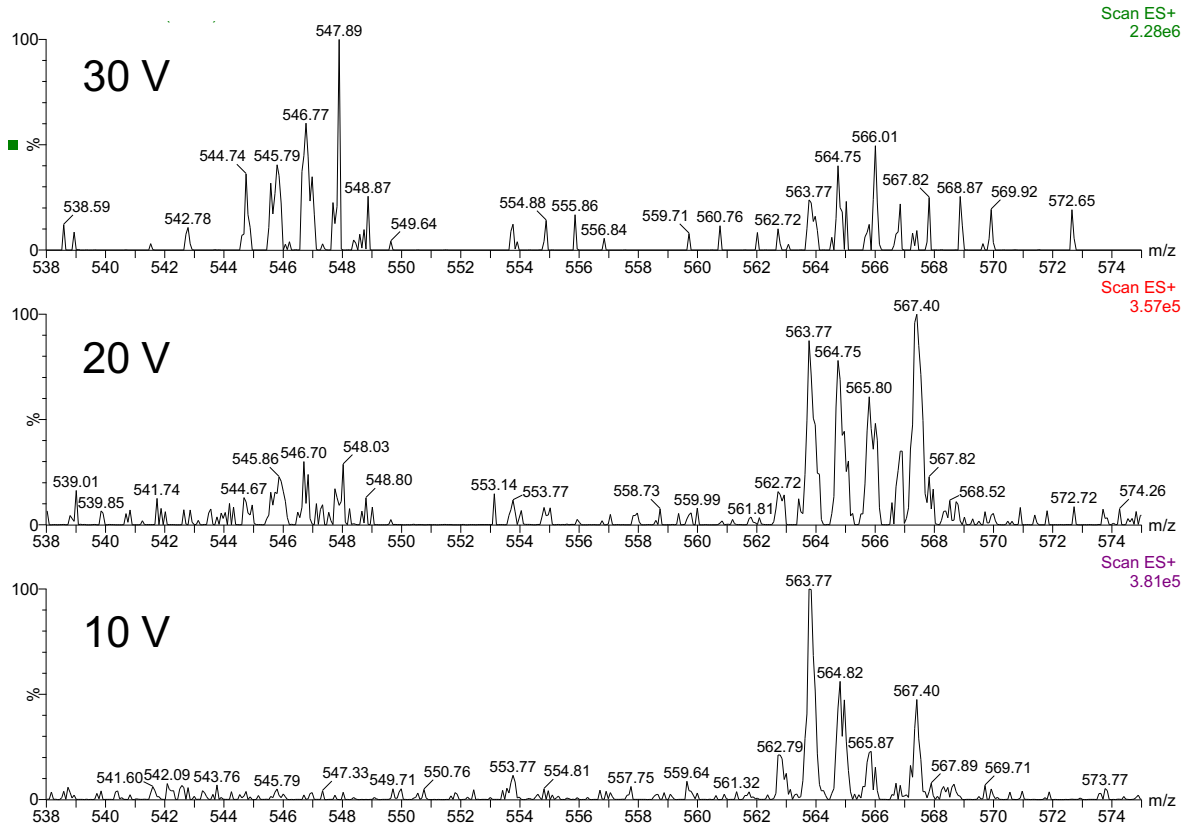

Figure S4. ESI$^+$ mass spectra of DOTA-EN-PBA ligand at different cone voltages: 30 V (top), 20 V (middle) and 10 V (bottom). The peaks around 563.3 m/z correspond to the mono-dehydrated adduct (M-H_2O+H^+); the peaks around 545.3 m/z correspond to the bis-dehydrated adduct (M-2H_2O+H^+).

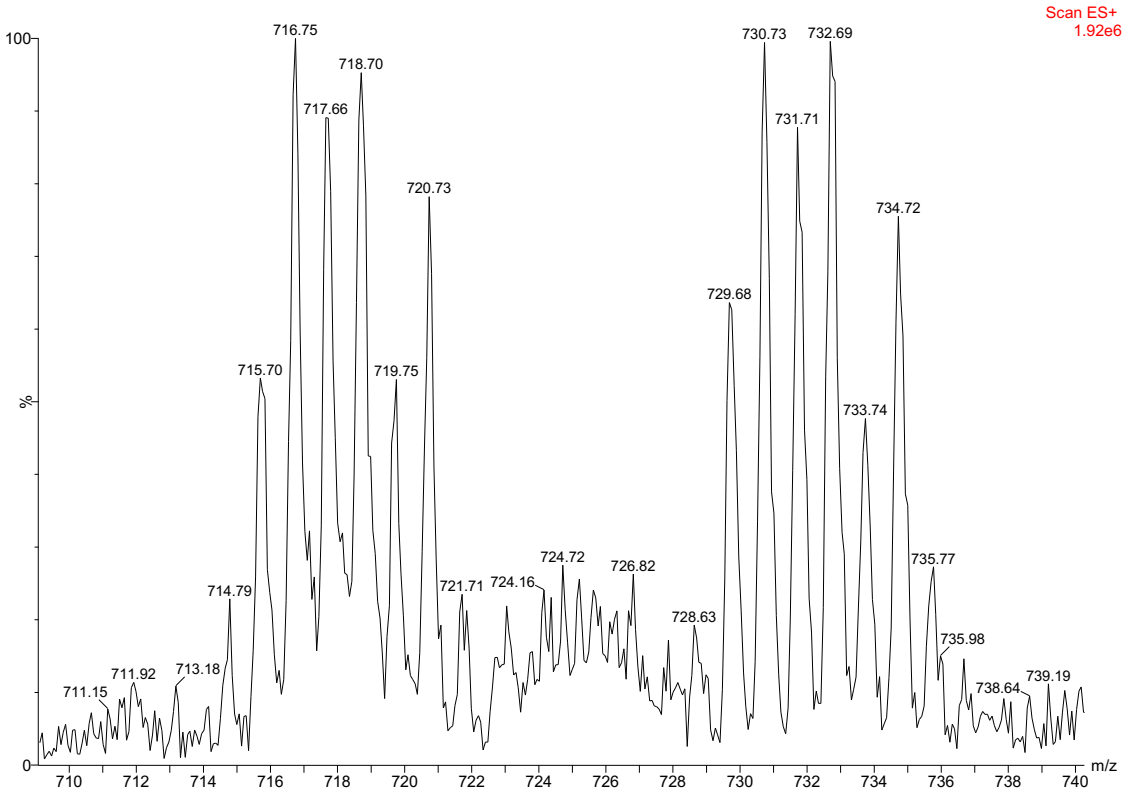

Figure S5. ESI$^+$ mass spectrum of GdDOTA-EN-PBA complex. Calculated for $[M+H]^+$ ($C_{25}H_{39}BGdN_6O_9^+$) = 736.2 m/z; for $M-H_2O+H^+$ ($C_{25}H_{38}BGdN_6O_8^+$) = 719.2 m/z.

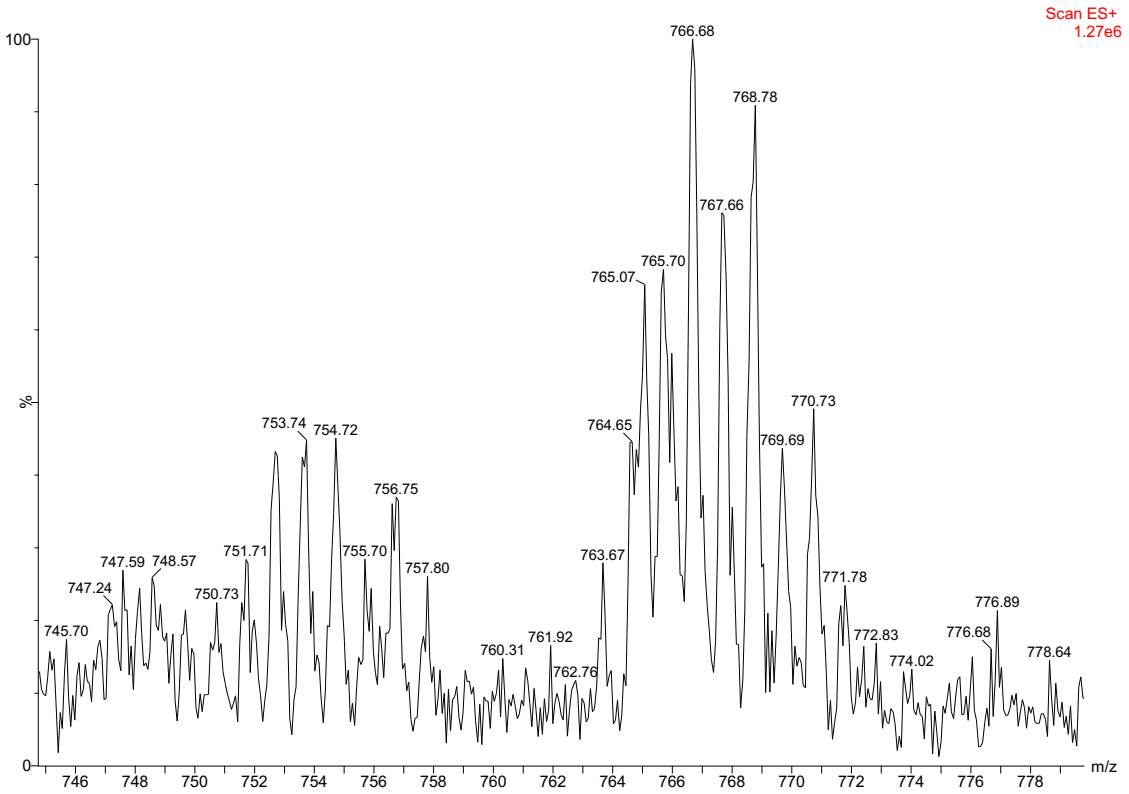

Figure S6. ESI$^+$ mass spectrum of GdDOTA-EN-F2PBA complex. Calculated for $M+H^+$ ($C_{25}H_{37}BF_2GdN_6O_9^+$) = 772.2 m/z; for $M-H_2O+H^+$ ($C_{25}H_{35}BF_2GdN_6O_8^+$) = 754.2 m/z.

3 NMR Spectra

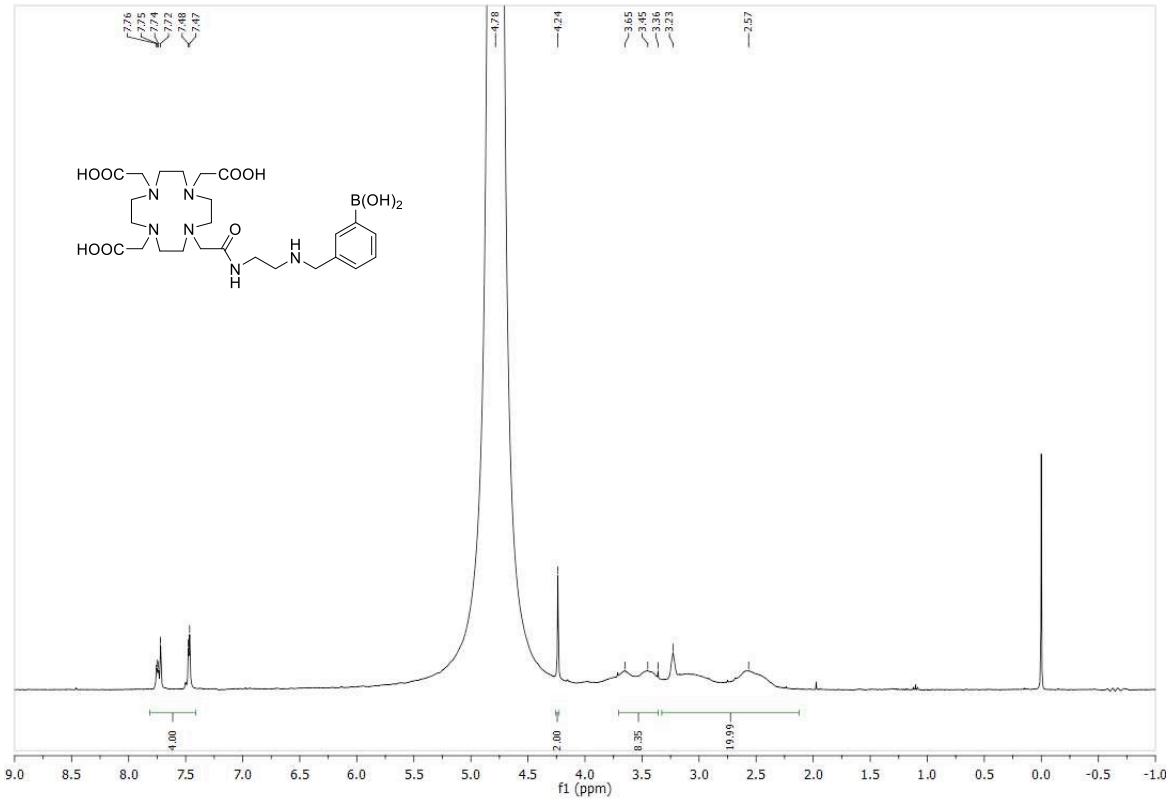

Figure S7. ^{1}H NMR spectrum in D_2O of DOTA-EN-PBA ligand prepared *via* solid-phase synthesis.

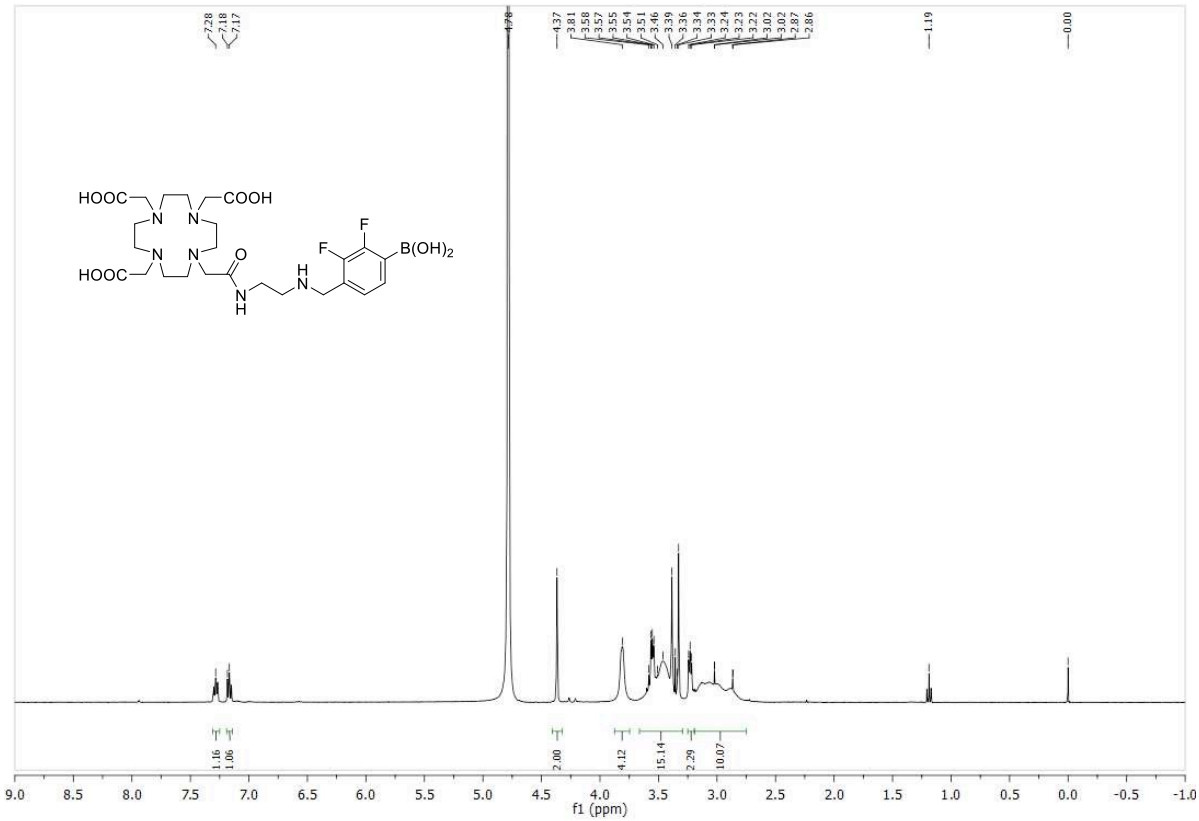

Figure S8. ^{1}H NMR spectrum in D_2O/CD_3CN of DOTA-EN-F2PBA ligand prepared *via* solid-phase synthesis. (residual Et_2O from precipitation is also observable).

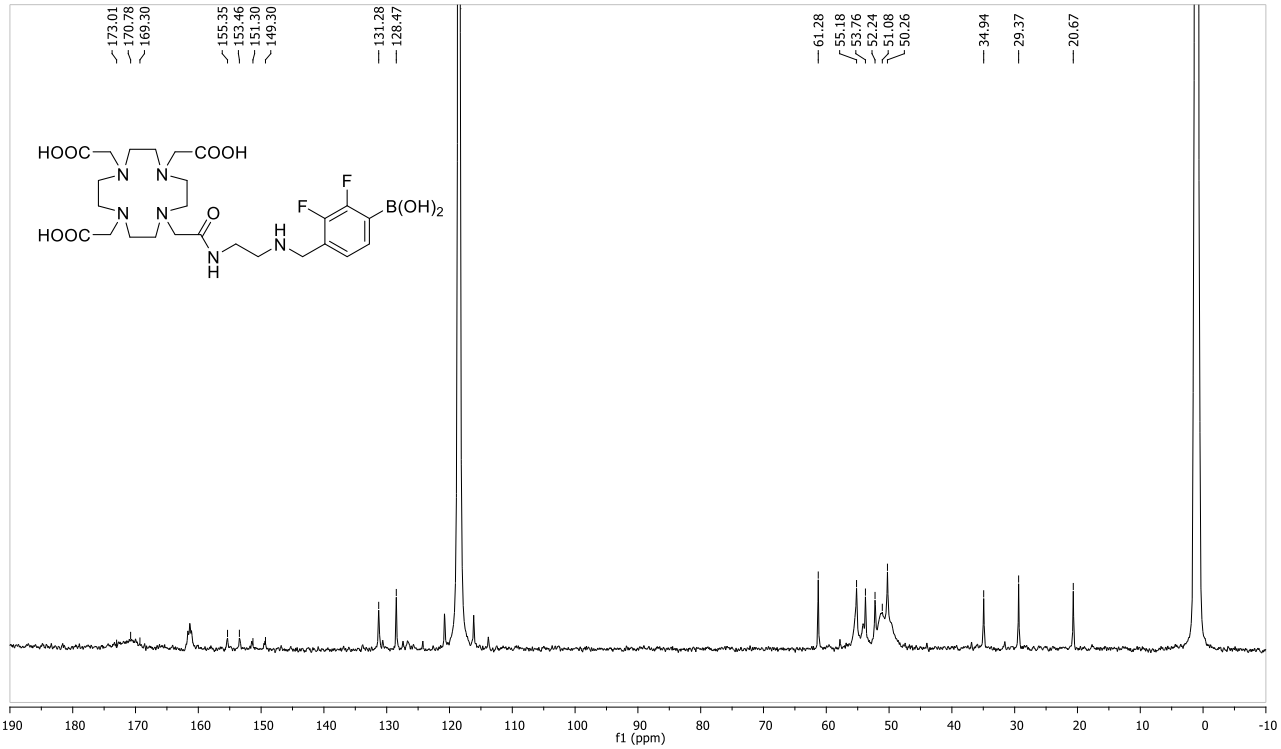

Figure S9. ^{13}C NMR spectrum in D_2O/CD_3CN of DOTA-EN-F2PBA ligand prepared *via* solid-phase synthesis (TFA as counterion is also observable).

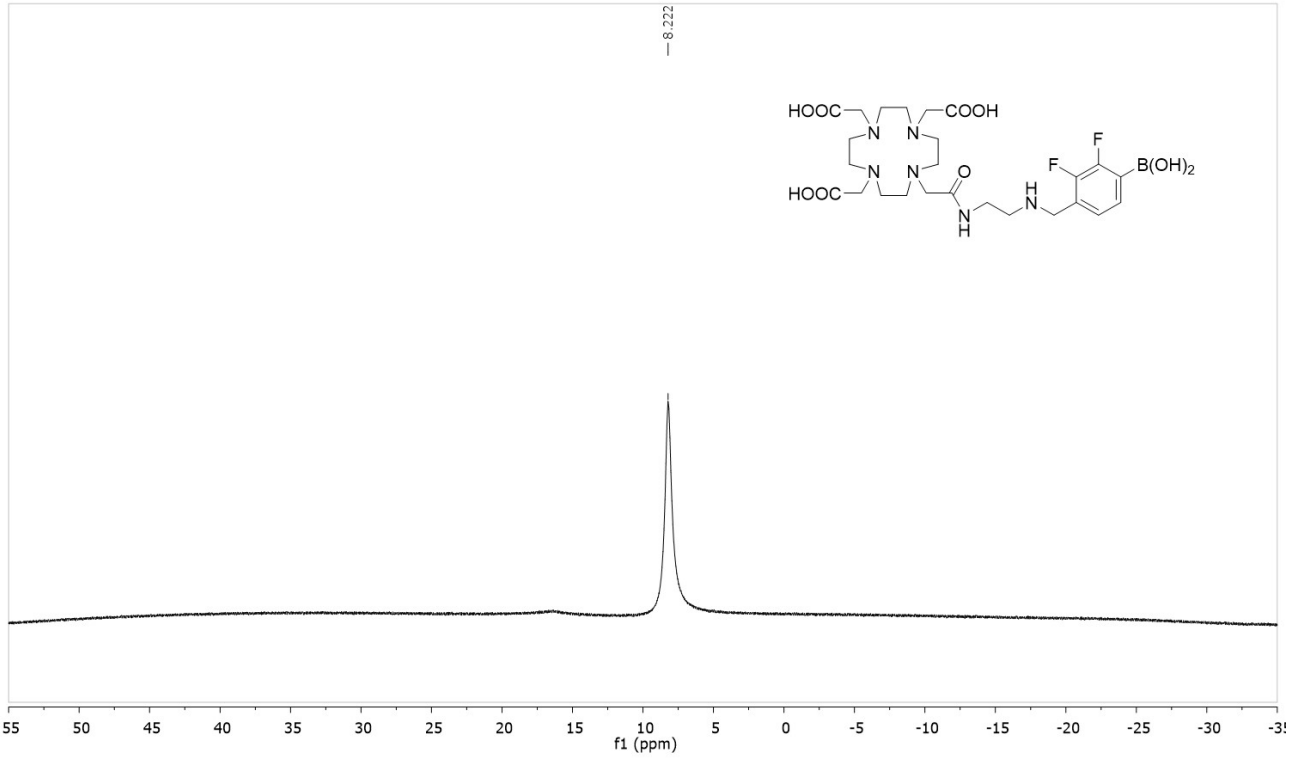

Figure S10. ^{11}B NMR spectrum in D_2O/CD_3CN of DOTA-EN-F2PBA ligand prepared *via* solid-phase synthesis.

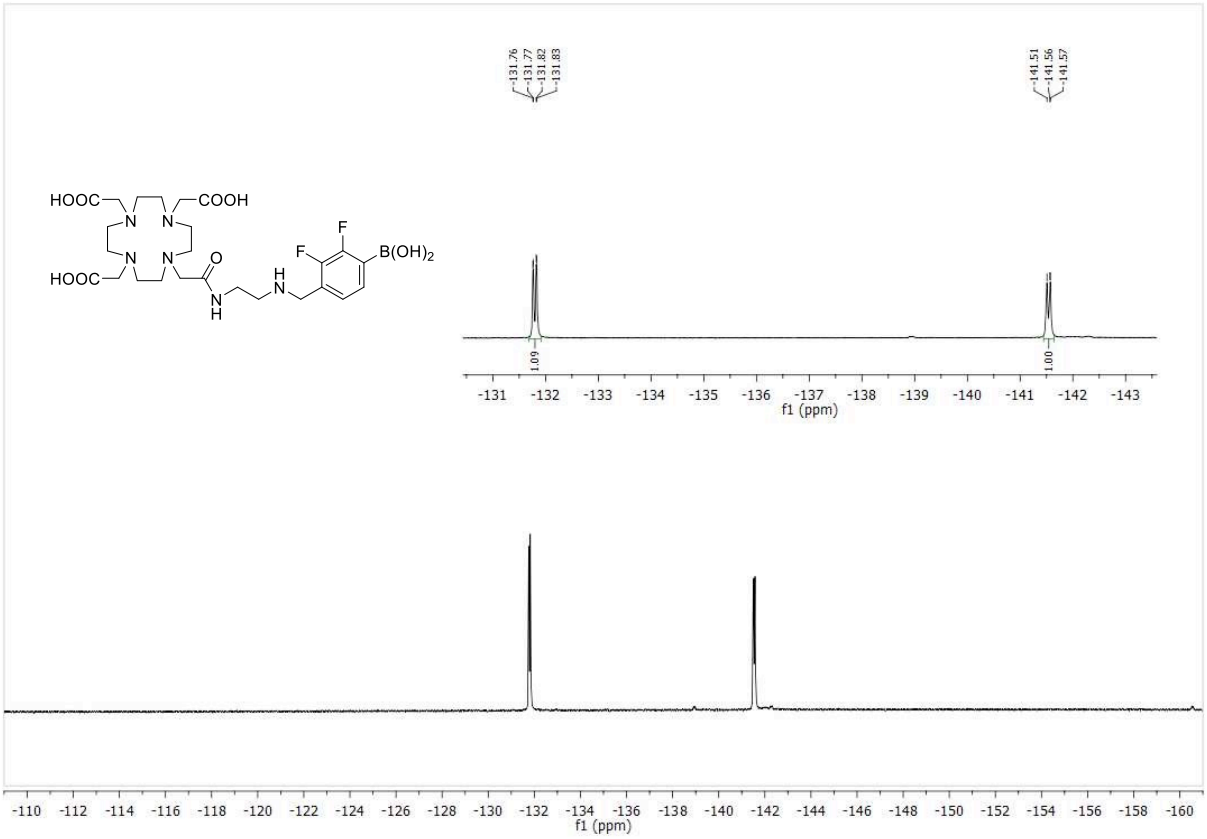

Figure S11. ^{19}F NMR spectrum in D_2O/CD_3CN of DOTA-EN-F2PBA ligand prepared *via* solid-phase synthesis.

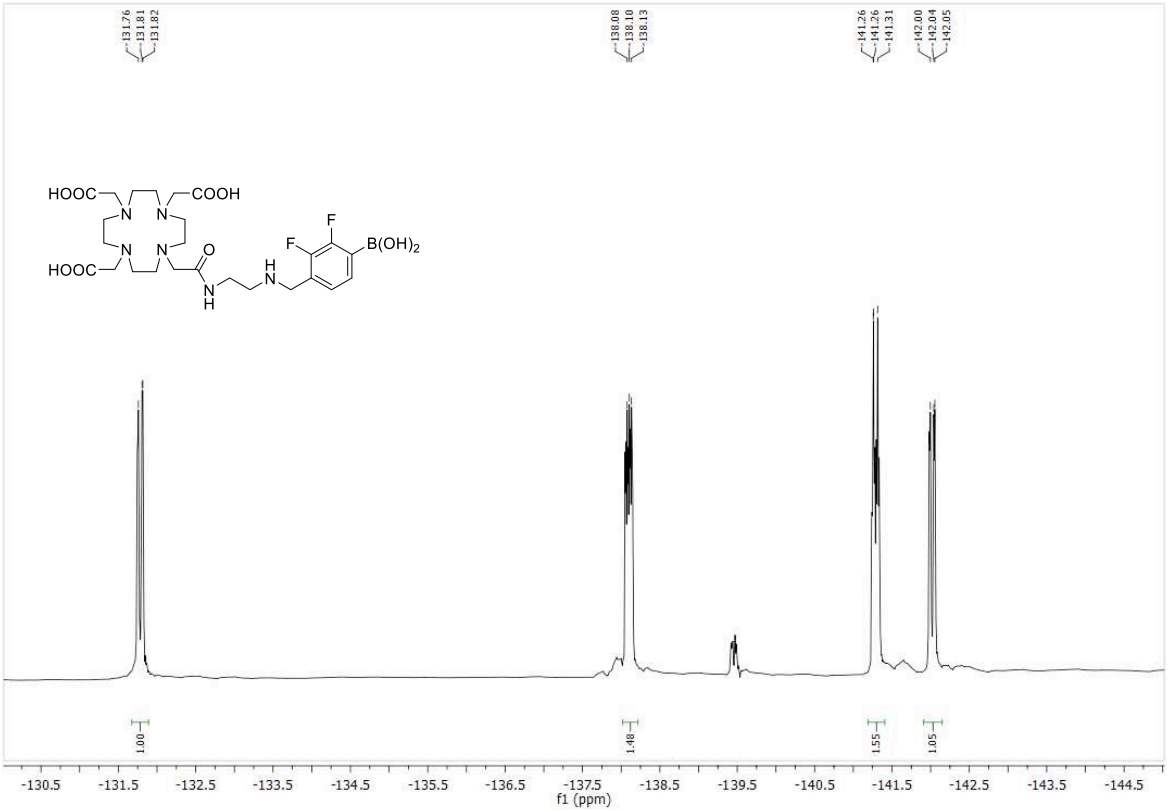

Figure S12. ^{19}F NMR spectrum in D_2O of DOTA-EN-F2PBA ligand prepared *via* liquid-phase synthesis. The integrals confirm the presence of two F-containing species with a ratio 1:1.5.

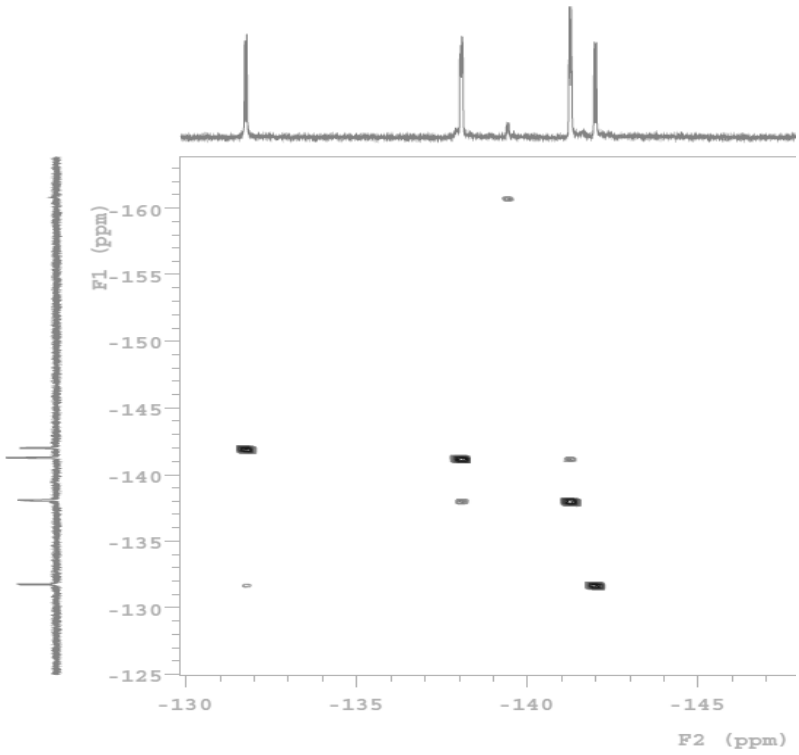

Figure S13. ^{19}F NMR COSY spectrum that identifies the two fluorine atoms belonging to each compound: -132 and -142 ppm for DOTA-EN-F2PBA and -138 and -141 ppm for its deboronated derivative.